Mem. S.A.It. Vol. 76, 810

Memorie della

The direct solar influence on climate: modeling the lower atmosphere

U. Cubasch[1], G. Bürger[1], I. Fast[1], Th. Spangehl[1] and S. Wagner[2]

[1] Metereologisches Institut, Freie Universität Berlin, Carl-Heinrich-Becker-Weg 6-10, D-12165 Berlin, Germany
e-mail: cubasch@zedat.fu-berlin.de
[2] Institut für Küstenforschung, GKSS, Max-Plank-Straße 1, D-21502 Geesthacht, Germany

Abstract. A set of ensemble experiments has been run focusing on the Dalton minimum to identify the individual contributions of solar variability, volcanism, greenhouse gas concentration changes and the combination of these forcing on climate. Additionally an idealized experiment has been carried out, where a sinusoidal forcing corresponding to the period of the Gleissberg-cycle, which led to the Dalton minimum, has been prescribed. Both, the volcanic and the solar forcing contribute to the global cooling during the Dalton minimum. The volcanic forcing, however, plays the major role for the global mean temperature. The temperature rise due to the greenhouse gases concentration increase counteracts this cooling only marginally. For the European region significant reduction of the solar constant (in the range of the imposed volcanic forcing) shift the NAO into the negative phase, thus enhancing the cooling over Europe. The experimental setup, which does not allow to take the volcanic aerosol forcing directly into consideration does not produce the winter warming in the years directly after the volcanic eruptions which has been seen in other modeling studies. In the idealized experiment the temperature follows the forcing with a lag of 4 to 6 years, which close to the observed value of 7 years. The MOC also reacts to the variations in the solar forcing. The pattern of the idealized response is only in the mid- and high latitudes similar to the one of the GHG experiments.

Key words. climate modeling, solar, volcanic, greenhouse gases forcings, NAO, Dalton Mimimum

1. Introduction

The attribution of the fluctuations of the global temperature during the last millennium, as it is given by instrumental observations (1850 to present) or through proxy reconstructions (past several centuries), to the main forcing factors (solar irradiance, volcanism, greenhouse gases) has been in discussion among the scientific community and the public. Particularly the solar intensity and the greenhouse gas concentrations showed significant amplifications during the 20^{th} century, parallel to the recorded global warming. This led to the question how much of that warming can be explained by either forcing. The literature gives different rates of explained variance (Friis-Christensen and Lassen 1991; Kelly and Wigley 1991; Schönwiese et al. 1994; Fligge et al. 1999;

Send offprint requests to: U. Cubasch

Thejll and Lassen 2000; Stott et al. 2003) which are based on different approximations of the solar activity and different databases for the Northern hemispheric temperature reconstruction.

To address the question, which part of the climate change has been caused by the individual forcings, the climate of the last millennium has been simulated in experiments using models of different complexity, which are forced with the historical variations of solar flux (S), volcanism (V) and greenhouse gases (G) (Crowley 2000; Bauer et al. 2003; Zorita et al. 2004; von Storch et al. 2004). Cubasch et al. (1997) found in numerical experiments that about 40% of the observed warming could be explained by solar forcing alone, Hegerl et al. (2003) were able to separate the greenhouse gas forcing, the solar forcing and the anthropogenic aerosol forcing. Tett et al. (1999) showed that only the combined influence of all forcings, that is, natural (S, V) and anthropogenic (G, sulphate aerosols), are able to explain the 20^{th} century temperature fluctuations adequately: While natural forcings seem to be mainly accountable for the mid-20^{th} century warming, anthropogenic factors dominate since about 1960 (see also Stott et al. 2000).

The Dalton Minimum of the early 19^{th} century (1790-1830) can be used to study the effect of the solar variability. In this preindustrial period greenhouse gases have only a small influence, while solar activity shows a strong negative anomaly (Hoyt and Schatten 1993; Lean et al. 1995). However, two major volcanic events (1809, 1815) also reduce the insolation during this time. Several temperature reconstructions (Jones et al. 1998; Briffa 2000; Briffa et al. 2001; Esper et al. 2002) point to a strong cold anomaly of the Northern hemisphere (NH). A reconstruction of North Atlantic Oscillation (Luterbacher et al. 2002) suggests low winter values between 1750 and 1830.

In the current paper a complex 3d coupled ocean-atmosphere model is employed to simulate the last 250 years with a combination of natural and anthropogenic forcings. After a description of the model and the experimental set-up (section 2), the model results are analyzed and compared to observations (section 3). In section 4, an idealized experiment is discussed in which the solar forcing is prescribed as a sine-wave. This section is followed by a summary (section 5).

2. The model and the experimental set-up

The climate model consists of the atmospheric model ECHAM4 with a horizontal spectral resolution of T30 (equivalent to 3.75° x 3.75°) and 19 vertical levels, coupled to the ocean model HOPE-G with a horizontal resolution of approx. 2.8° x 2.8° with equator refinement and 20 vertical levels. The ocean and atmosphere models are coupled through flux adjustment to avoid climate drift in long climate simulations.

The experiments are based on an experiment described in von Storch et al. (2004), i.e. a 1000 year simulation (often referred to as ERIK simulation), in which the model was driven by estimations of past variations of the solar constant, volcanic activity and concentrations of greenhouse gases (Figure 1). Annual values of net radiative forcing due to solar variability and volcanic activity were calculated by Crowley (2000) from concentrations of ^{10}Be (a cosmogenic isotope), historical observations of sun spots and acidity measurements in ice cores. In these simulations, they were translated to variations of an effective solar constant communicated to the climate model, represented by a global annual number, equally distributed over the solar spectrum, with no seasonal or geographical dependence. Thus, the solar and volcanic forcings differ by their amplitudes and time evolution only. Atmospheric concentrations of greenhouse gases were derived from air bubbles trapped in polar ice cores (Etheridge et al. 1996; Blunier et al. 1995). Changes in tropospheric sulphate aerosols and ozone concentrations have not been included.

Table 1. List of transient experiments S: solar, V: volcanic, G: greenhouse gases and their possible combinations. CTL: control experiment with all forcings set constant. T: time-varying forcing taken from von Storch et al. (2004)

Forcing	CTL	S	V	G	SV	SG	VG	SVG
CO_2 (ppm)	280	280	280	T	280	T	T	T
CH_4 (ppb)	700	700	700	T	700	T	T	T
N_2O (ppb)	265	265	265	T	265	T	T	T
Solar Constant (W/m^2)	1365.0	T	1365.0	1365.0	T	T	1364.6	T
Volcanism	–	–	T	–	T	–	T	T

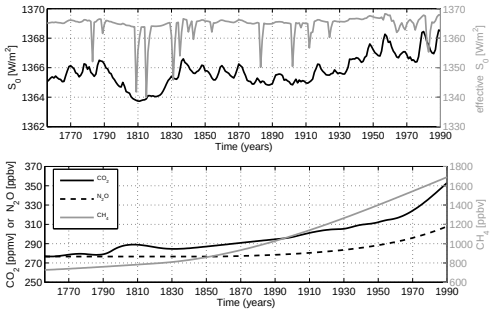

Fig. 1. Top: The temporal evolution of the natural forcing (solar forcing: black, effective solar forcing:=solar constant and volcanism: gray). Note that only the tropospheric portion of the volcanic aerosol forcing is taken into account. Bottom: The temporal evolution of the greenhouse gases concentrations.

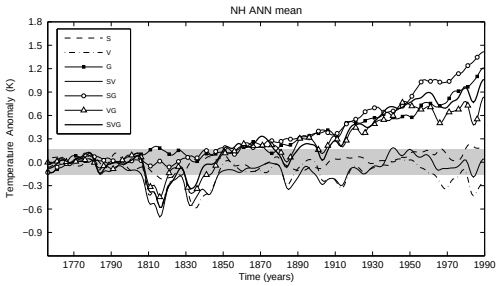

Fig. 2. Decadally smoothed simulated annual Northern hemisphere mean surface air temperature anomalies for the 7 experiments relative to the years 1756 to 1789. The grey band indicates the uncertainty given by the climate noise estimated as twofold standard deviation in the control experiment.

3. The impact of external natural and anthropogenic forcing

Starting from the year 1756 of the ERIK experiment, a number of experiments have been run, in which the solar (S), the volcanic (V) and the greenhouse gas (G) forcing have been switched on and off (Table 1). Each experiment consists of an ensemble of 3. The ensemble was generated by taking the initial conditions from years with similar global mean temperature of the von Storch et al. (2004) simulation. The last 235 years of the experiment by von Storch et al. (2004) together with two more experiments starting in the year 1756 form the experiment SVG.

3.1. Northern hemisphere near surface temperature response

Figure 2 shows for the period from 1756 to 1990 the ensemble annual mean temperatures, as simulated from all possible combinations of the forcings S, V, and G.

Significant cooling events coincide with outbreaks of volcanoes. In the most recent decades all simulations that include the greenhouse gases increase are warmer than the experiments driven only by natural climate forcing. During the late 20^{th} century the negative volcanic forcing and increased solar irradiance act against each other, so that temperature changes in the natural run are mainly limited to

Table 2. Coherence between simulations and observations (CRUTEM2v - www.cru.uea.ac.uk/ftpdata/crutem2v.nc) at a timescale of 5 years (using the maximum entropy method). For annual values (ANN), SVG shows highest coherence followed by VG and S. This is similar for winter (DJF), only that G values are somewhat larger. For summer (JJA), the coherence is generally reduced, with largest values for SV.

	S	V	G	SV	SG	VG	SVG
ANN	0.72	0.21	0.62	0.64	0.53	0.75	0.81
DJF	0.59	0.06	0.75	0.28	0.69	0.69	0.80
JJA	0.27	0.32	0.11	0.63	0.04	0.34	0.42

the range of internal variability given by control run.

The temperature increase is stronger in the simulation SVG than in the observations. This discrepancy is more pronounced during summer than in winter, which indicates that it is caused by the missing representation of the aerosols in the model.

All simulations show enhanced coherence with the observed record towards the longer time scales (Table 2). While for the winter season experiment SVG has the highest values followed by G, SG and VG (which mainly represents the warming trend), greenhouse gases seem to be of less importance for the summer season; here the combined solar and volcanic effects seem to be more important.

3.2. Regional temperature anomalies

The following discussion concentrates on the experiments with the single forcing G, S, and V, and the natural forcing SV, which is complementary to the study of Wagner and Zorita (2005), which analyzed the response in the SVG, SG and VG experiments.

In winter, the G simulation shows a slight warming during the Dalton Minimum, which is possibly a response to the stepwise increase of the GHG-concentration during this period (Figure 3). The volcanic and natural experiments show a significant cooling in the low latitudes and over northern Europe and northern Asia. This cooling is found to be comparatively strong in V and SV, where the cooling signal extends over the Arctic regions, while the S experiment mainly displays a cooling over Eurasian high and middle latitudes. An insignificant cooling or even a warming can be found west of Greenland and over North America. The simulated temperature anomalies southeast of Greenland are found to be consistent with the inverse of the GHG warming signal (Cubasch et al, 2001), which shows a marginal warming or even cooling. In the GHG simulations it can be connected to a decline of the meridional overturning circulation (MOC). Consistent with this the S and V experiments exhibit a weak anti-correlation to the MOC.

The near surface temperature pattern with a cooling over northern Europe and Asia and warming over North America and west of Greenland can be related to the NAO variability found in observations (van Loon and Rogers 1978; Hurrel 1995). The simulated NAO variability is assessed by means of empirical orthogonal function (EOF) analysis based on winter mean sea level pressure (MSLP) fields for the sector covering the Northern hemisphere from 110° W to 70° E and 20° to 90° N. The first EOF explains 39% of the total MSLP variance in the control experiment. The pattern is very robust and independent of the forcings. The NAO indices are calculated by projection of the winter MSLP fields onto the first EOF pattern of the corresponding simulation. An EOF analysis was also applied to the mean winter near surface temperature fields. The first EOF, which strongly resembles the NAO-related temperature pattern, explains 24% of the total near surface temperature variance in the control experiment. The first principal components (PCs) of MSLP and near surface temperature are highly correlated in all simulations (linear correlation coefficient around 0.7) indicating that the model is able to reproduce the well known relationship between the NAO and European winter temperature variability (EOF patterns not shown).

A distinct NAO signal can be seen in winters starting in the year of an volcanic eruption (0^{th} winter) and the 1^{st} winter after a volcanic eruption (Figure 4): here one finds a clear shift

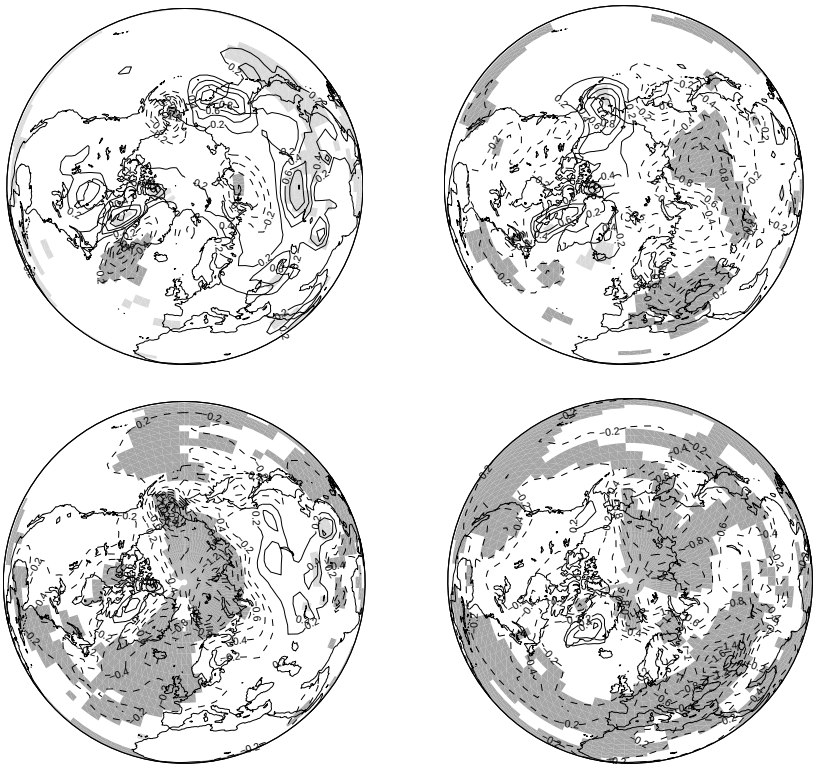

Fig. 3. The simulated winter (DJF) temperature anomalies for the Dalton Minimum (1790-1830). Top left: GHG experiment, top right: solar experiment, bottom left: volcanic experiment, bottom right: natural (solar + volcanic) experiment. Anomalies refer to the period from 1756 to 1789. Contour interval is 0.2 K. Shaded areas are significant above the 95^{th} percentile value after t-test.

of the NAO into the negative phase which is accompanied by a cooling over Europe. The NAO and temperature response to the volcanic forcing vanish already in the 2^{nd} winter after the eruption. This behaviour is in contrast to a number of other studies which find a northern European warming, i.e. a positive NAO, in the winter after a volcanic eruption (e.g. Kirchner et al. 1999; Shindell et al. 2003; Yoshimori et al. 2005). While the first two authors link this to the warming in the tropical low stratosphere due to absorption of near-infrared radiation by volcanic aerosols, which is not implemented in our simulation, Yoshimori simulates a winter warming and a positive NAO even without explicitly calculating the stratospheric aerosol forcing, because the sea ice edge is extended to the south after an eruption and the synoptic activity along its southern flanks is enhanced. Our result (i.e. the negative NAO response to decreases in the effective solar constant) is consistent with the reversal of the behaviour of the NAO in the global warming simulations, where the NAO tends to become more positive with increased forcing (cf. Paeth et al. 1999). Note that a weakening of the westerlies as found in our simulations is consistent with the concept of reduced meridional temperature gradients in the upper troposphere in a colder climate.

During the Dalton Minimum (1790-1830), an increased incidence of the negative phase of the NAO is found in both, the solar (58%) and volcanic experiments (59%) (Table 3). This shift of the NAO into the negative phase is found to be significant on the 90% level after a χ^2-test. If shifts in the NAO were deterministi-

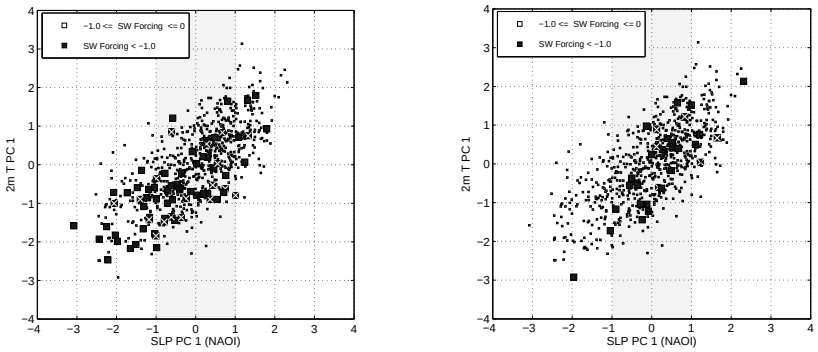

Fig. 4. The dynamic model winter (DJF) response to volcanic forcing. The scatter plots show the principal component values of the leading winter modes for the surface air temperature and MSLP respectively. Results are based on the full volcanic forcing ensemble (3 simulations). The linear correlation coefficient is 0.7. Black squares indicate that the volcanic forcing exceeds -1.0 W/m^2 (this corresponds to the reduction of the solar constant of approx. 5.7 W/m^2). Left: year 0 and 1 after the eruption; winter seasons during the Dalton Minimum (1790-1830) with major volcanic forcing are marked by a white cross. Right: year 2 after the eruption.

Table 3. The relative frequency of negative low-pass filtered NAO indices during the Dalton Minimum (in brackets: for the whole simulated period 1756-1990). Statistically significant values at the 90% level are in bold (based on χ^2-test).

Experiment	NAO-negative (detrended data)
S	**58%** (48%)
V	**59%** (49%)
SV	48% (48%)

cally driven by the forcing, the natural simulation (SV) should have an even stronger signal; but this is not the case (48%). The internal variability of the system is so large that the sample of three used in this study is not sufficient to isolate a clear signal.

4. Idealized solar forcing experiment

Another method of generating a large sample is to run long experiments with cyclic forcing. This method has been applied to identify the Gleissberg cycle with a periodicity of approx. 80 years. In the reconstructed solar datasets of Lean et al. (1995) and Hoyt and Schatten (1993) this cycle emerges only 3 times. In the setup introduced here, the model was forced by 10 sinusoidal cycles of period 76y (=760y) and an amplitude of 5 W/m^2 at the top of the atmosphere mimicking the range of solar constant changes since 1610 in the reconstruction of Hoyt and Schatten (1993). This simulation is referred to as S76.

Figure 5 shows the forcing together with the global mean near surface temperature response. The temperature closely follows the forcing, with variations of about 0.6-0.8 K. The cross-correlations shown in Figure 6 show a maximum of about 0.7 at a lag of 4-5 years, which is slightly smaller than previous estimates (Cubasch et al. 1997). Note that the other experiments including a solar forcing component (i.e. S, SV, SG, SVG) have smaller correlations and a weaker dependence on the lag, pointing to a clearer dynamic response for S76. The observations have a maximum correlation at lag of about 7 years.

As a spatial response pattern we show the point-wise correlation for the lag of 5y in Figure 7. The pattern is quite similar for S76 and SVG (Table 4) with highest correlations over the tropical Atlantic and Indic, and decreasing values towards higher latitudes (as in Cubasch et al. 1997). The overall response is

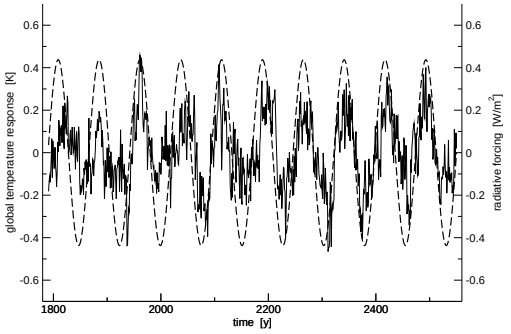

Fig. 5. The sinusoidal solar forcing with a period of 76 years (dashed line) and the models response in the near-surface temperature (solid line)

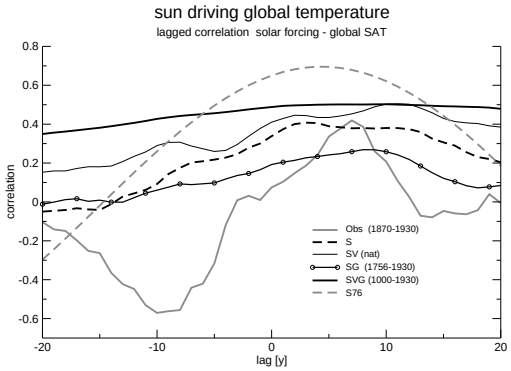

Fig. 6. Lagged correlations between solar forcing (idealized for S76 or reconstructed) and global surface temperature response. S76 (dashed grey) reveals the sharpest response, with a maximum correlation of 0.7 at lag 5y. The response of the other simulations is similar but more disturbed, mainly by low-frequency noise, especially SVG (black). Besides this, sampling errors also obscure the response estimated from instrumental observations: While a positive peak at lag 7y points to a response similar to the simulations, a negative, and stronger, peak appears at lag -10y, which is counterintuitive.

similar for S and SV, but with much stronger negative correlations for the high latitudes. The pattern is quite different from the pattern obtained for the GHG-experiment over wide areas of the tropical oceans, while it is similar in the mid-latitudes and polar regions.

In all experiments, anti-correlations in the North Atlantic area of deep convection point to an influence of solar heating on the meridional

Table 4. Pattern correlation between the response patterns of the various experiments which used variable solar forcing.

	S	SV	SG	SVG	S76
OBS	-0.15	-0.05	-0.08	-0.09	-0.08
S		0.37	0.63	0.70	0.49
SV			0.66	0.61	0.69
SG				0.87	0.76
SVG					0.75

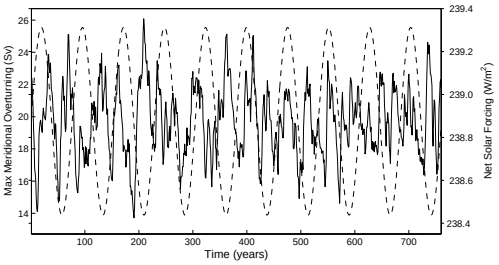

Fig. 8. The sinusoidal solar forcing with a period of 76 years (dashed line) and the maximum meridional overturning in the North Atlantic (solid line).

overturning circulation (MOC). The time series of maximum Atlantic overturning (Figure 8) is, however, only weakly associated with the global temperature with negative cross correlations never exceeding 0.3 at a lag between 7 to 10 years. This is weaker than previously reported (Cubasch et al. 1997).

5. Summary

Ensemble experiments with three members have been run focusing on the Dalton Minimum to identify the individual contributions of solar variability, volcanism, greenhouse gas concentration changes and the combination of these forcing on climate. As the sample size proved not sufficient to obtain a well defined response signal in all cases, an idealized experiment with 760 years simulation time has been run, where a sinusoidal forcing corresponding to the periods of the Gleissberg-cycle with a period of 76 years

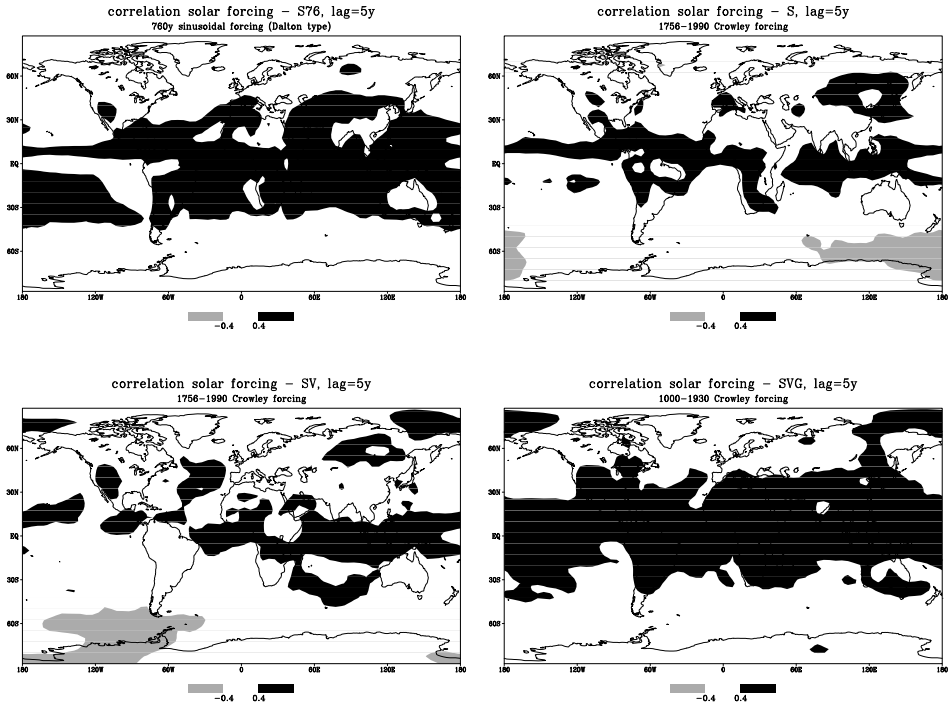

Fig. 7. Pointwise correlation between solar forcing and near surface temperature, of S76 and S (upper left and right) and SV and SVG (lower left and right). High positive correlations (≥ 0.4) appear throughout in the tropical band, mainly over the oceans (dark shaded areas), whereas negative correlations ($\leq$ -0.4) dominate in the Southern Oceans (grey shaded areas). The temperature data have been low-pass filtered (> 5y) to remove ENSO variability.

(which led to the Dalton Minimum) has been prescribed.

In the ensemble experiments, both, the volcanic and the solar forcing contribute to the global cooling during the Dalton Minimum. The volcanic forcing, however, plays the major role for the global mean temperature. The temperature rise due to the greenhouse gases concentration increase counteracts this cooling only marginally.

For the European region significant reduction of the solar constant (i.e. in the range of the imposed volcanic forcing) shift the NAO into the negative phase, thus enhancing the cooling over Europe. The experimental setup, which does not allow to take the volcanic aerosol forcing directly into consideration, but prescribes its first order effect as a reduction of the solar input, does not produce the winter warming in the years directly after the volcanic eruptions which has been seen in other modeling studies. This means that it shows the inverse response found in GHG increase simulations.

In the idealized experiment the global mean temperature follows the forcing with a lag of 4 to 6 years, which close to the observed value of 7 years. The response is not completely sinusoidal, but noisy and shows in some cases in the cooling phase a hesitation before cooling down to the minimum. The pattern of the idealized response is only in the mid- and high latitudes similar to the one of the GHG experiments. Here the MOC reacts to the variations in the solar forcing similarly as the GHG-experiments, i.e. with a weakening at high levels of insolation and a strengthening at low levels of insolation. in the idealized experiments a response pattern encompassing the tropics and

subtropics emerges which is particularly visible in the idealized forcing experiment.

Acknowledgements. E. Zorita and F. Gonzalez-Rouco for providing the ERIK experiment. Part of this research was funded under the EU projects SOAP and ENSEMBLES. The model experiments were carried out at the DKRZ.

References

Bauer, E., Claussen, M., Brovkin, V., & Huenerbein, A. 2003, Geophys. Res. Lett., 30 (6), doi: 10.1029/2002GL016639

Blunier, T., Chappellaz, J.A., Schwander, J., Stauffer, B., & Raynaud, D., 1995, Nature, 374, 46

Briffa, K.R., 2000, Quat. Sci. Rev., 19, 87

Briffa, K.R., Osborn, T.J., Schweingruber, F.H., Harris, I.C., Jones, P.D., Shiyatov, S.G., & Vaganov, E.A., 2001, J. Geophys. Res., 106, 2929

Crowley, T.J., 2000, Science, 289, 270

Cubasch, U., Hegerl, G.C., Voss, R., Waszkewitz, J., & Crowley, T.C. 1997, Clim. Dyn., 13, 757

Cubasch, U., Meehl, G.A., Boer, G.J., Stouffer, R.J., Dix, M., Noda, A., Senior, C.A., Raper, S., & Yap, K.S., 2001, In: Climate Change 2001: The Scientific Basis. Contribution of Working Group I to the Third Assessment Report of the Intergovernmental Panel on Climate Change [Houghton, J. T., Ding, Y., Griggs, D.J., Noguer, M., van der Linden, P., Dai, X., Maskell, K., Johnson, C.I. (eds.)]. Cambridge University Press, ISBN 0521 01495 6

Esper, J., Edward, R.C., & Schweingruber, F.H., 2002, Science, 295, 2250

Etheridge, D., Steele, L.P., Langenfelds, R.L., Francey, R.J., Barnola, J.M., & Morgan, V.I., 1996, J. Geophys. Res., 101, 4115

Fligge, M., Solanki, S.K., & Beer, J., 1999, Astron. and Astrophys. , 346, 313

Friis-Christensen, E., & Lassen, K., 1991, Science, 254, 698

Hegerl, G.C., Crowley, T.J., Baum, S.K., Kim, K., & Hyde, W.T., 2003, Geop. Res. Let., 30 (5), 1242, doi:10.1029/2002GL016635

Hurrel, J.W., 1995, Science, 269, 676

Hoyt, D.V., & Schatten, K.H., 1993, J. Geophys. Res., 98, 18895

Jones, P.D., Briffa, K.R., Barnett, T.P., & Tett, S.F.B., 1998, The Holocene, 8, 455

Kelly, P.M., & Wigley, T.M.L., 1991, Nature, 360, 328

Kirchner, I., Stenchikov, G.L., Graf, H.-F., Robock, A., & Antuna, J.C., 1999, JGR, 104, 19039

Lean, J., Beer, J., & Bradley, R., 1995, Geophys. Res. Lett., 22, 3195

Luterbacher, J., Xoplaki, E., Dietrich, D., Jones, P.D., Davies, T.D., Portis, D., Gonzalez-Rouco, J.F., von Storch, H., Gyalistras, D., Casty, C., & Wanner, H., 2002, Atmospheric Science Letters, doi:10.1006/asle.2001.0044

Paeth, H., Hense, A., Glowienka-Hense, R., Voss, R., & Cubasch, U., 1999, Climate Dynamics, 15, 953

Schnwiese, C.-D., Ullrich, R., Beck, F., & Rapp, J., 1994, Climatic Change, 27, 259

Shindell, D.T., Schmidt, G.A., Miller, R.L., & Mann, M.E., 2003, Journal of Climate, 16, 4094

Stott, P.A., Tett, S.F.B, Jones, G.S., Allen, M.R., Mitchell, J.F.B., & Jenkins, G.J., 2000, Science, 15, 2133

Stott, P.A., Jones, G.S., & Mitchell, J.F.B., 2003, J. Climate, 16 (24), 4079

Tett, S.F.B., Stott, P.A., Allen, M.A., Ingram W.J., & Mitchell, J.F.B., 1999, Nature, 399, 569

Thejll, P.A., & Lassen, K., 2000, J. of Solar-Terrestrial Physics, 13, 1207

Van Loon, H., & Rogers, J.C., 1978, Mon. Wea. Rev., 106, 296

Von Storch, H., Zorita, E., Jones, J.M., Dimitriev, Y., Gonzales-Rouco, F., & Tett, S.F.B., 2004, Science, 306, 769

Wagner, S., & E. Zorita, 2005, Clim. Dyn, online first

Yoshimori, M., Stocker, T.M., Raible, C.C., & Renold, M., 2005, J. Climate, in press

Zorita, E., von Storch, H., Gonzalez-Rouco, F., Cubasch, U., Luterbacher, J., Legutke, S., Fischer-Bruns, I., & Schlese, U., 2004, Meteorologische Zeitschrift, Meteor. Z. 13, 271